ACS Photonics

pubs.acs.org/journal/apchd5

Letter

Plug-and-Play Molecular Approach for Room Temperature Polariton Condensation

Prathmesh Deshmukh, Sitakanta Satapathy,* Evripidis Michail, Andrew H. Olsson, Rezlind Bushati, Ravindra Kumar Yadav, Mandeep Khatoniar, Junsheng Chen, George John, Bo W. Laursen, Amar H. Flood, Matthew Y. Sfeir, and Vinod M. Menon*

Cite This: *ACS Photonics* 2024, 11, 348−355

Read Online

ACCESS | Metrics & More | Article Recommendations | Supporting Information

Downloaded via INDIANA UNIV BLOOMINGTON on March 4, 2024 at 17:24:30 (UTC).
See https://pubs.acs.org/sharingguidelines for options on how to legitimately share published articles.

ABSTRACT: Exciton-polaritons (EP), half-light half-matter quasiparticles that form in optical cavities, are attractive platforms for creating macroscopic coherent states such as Bose−Einstein condensation (BEC). EPs based on organic molecules are of particular interest for realizing such states at room temperature while offering the promise of synthetic tunability. However, the demonstrations of such condensates have been limited to a few specific molecular systems (Keeling et al. Bose-Einstein condensation of exciton-polaritons in organic microcavities. *Annual Review of Physical Chemistry* **2020**, *71*, 435−459). Here we report a universal platform for realizing molecular polariton condensates using commercial dyes that solve long-standing material challenges. This solution is made possible using a new and programmable molecular material called small-molecule, ionic isolation lattices (SMILES) with the potential to incorporate a wide array of molecular fluorophores (Benson et al. Plug-and-Play Optical Materials from Fluorescent Dyes and Macrocycles. *Chem* **2020**, *6*, 1978−1997). We show EP condensation in rhodamine by incorporating it into a SMILES lattice placed in a planar microcavity. The SMILES approach overcomes the major drawbacks of organic molecular photophysical systems, such as self-quenching, which sets the foundation for realizing practical polaritonic devices operating at ambient temperatures covering a wide spectral range.

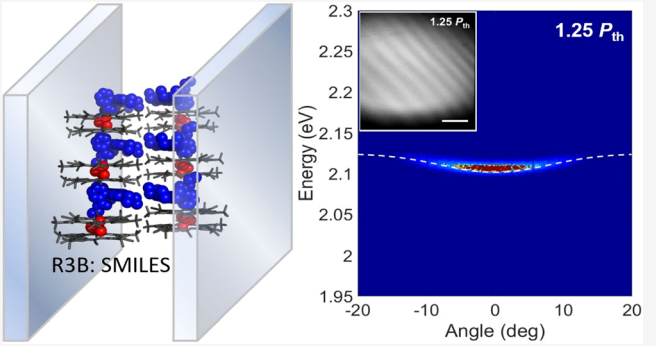

KEYWORDS: *exciton-polaritons, organic dyes, molecular engineering, programmable materials, polariton lasing, Bose−Einstein condensation*

INTRODUCTION

EP condensates have become a platform for both fundamental investigations and technological developments.[3,4] Owing to their smaller effective mass, EPs have the advantage of realizing Bose−Einstein condensation (BEC) at elevated temperatures. While not true BECs, since they are not at thermal equilibrium, they exhibit some of the novel features like superfluidity[5,6] and, by analogy to cold atom lattices, can be implemented as Hamiltonian emulators.[7] These properties motivate the exploration and critical evaluation of new optical materials to support EP condensation. To this end, we report the first use of small-molecule, ionic isolation lattices[2] (SMILES, Figure 1a) that promise to incorporate commercially available organic fluorophores directly and easily into optical devices for EP condensation.

There have been different material platforms that show polariton condensation at room temperature, such as wide band gap semiconductors, 2D materials, perovskites, and organic molecular solids.[1,8−11] While early experiments used inorganic semiconductors hosting Wannier excitons,[12] for over a decade now there has been much interest in realizing condensation using large binding energy Frenkel excitons in organic molecular solids.[1,13] The organic molecular systems have garnered much attention owing to the promise of on-demand synthetic tunability, whether for materials compatibility or control of photophysical properties, as well as their potential integration with flexible substrates. Despite this promise, the demonstrations to date have been carried out using only a few specific systems ranging from single crystals to ladder type polymers and fluorescent proteins.[1,13−21] It would be ideal if we could instead choose from the large body of organic fluorescent dyes available today to truly unleash the synthetic power of organic fluorophores.

Received: October 27, 2023
Revised: December 12, 2023
Accepted: January 9, 2024
Published: January 25, 2024

© 2024 American Chemical Society

https://doi.org/10.1021/acsphotonics.3c01547
ACS Photonics 2024, 11, 348−355

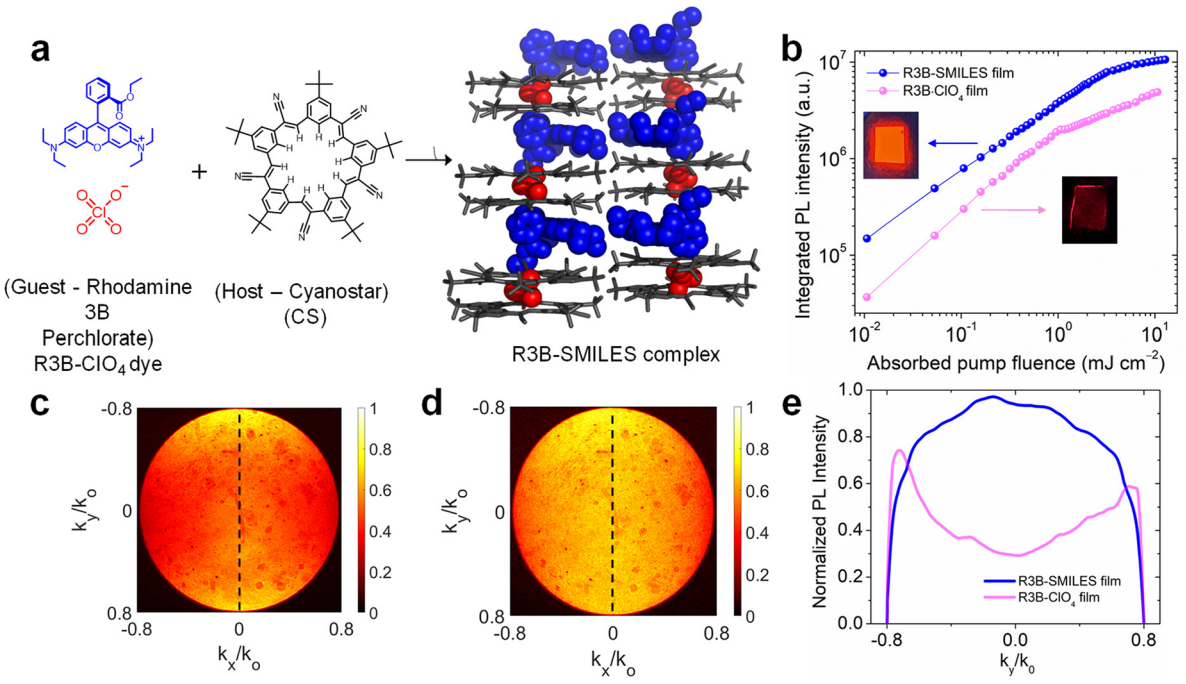

Figure 1. Materials and thin film characterization. (a) Chemical structure of the reactant precursors and R3B-SMILES material. (b) Power-dependent photoluminescence (PL) intensity comparison for thin PMMA films incorporating R3B alone (10 mM in R3B) and R3B-SMILES (10 mM in R3B). Inset shows the PL from the respective films, showing a much brighter SMILES film. Experimental momentum resolved PL showing intensity distribution at the back focal plane (momentum space) for the (c) R3B and (d) R3B-SMILES films along with (e) a comparison of the linecut of the PL plots along the vertical direction at $k_x = 0$. The maximum in the R3B-SMILES (blue) occurs at $k_y = 0$, indicative of in-plane dipoles as opposed to the bare dye (magenta) showing maximal PL at large in-plane momentum values ($k_y = 0.8$) typical for out-of-plane dipoles.

Realization of EP condensation from any arbitrary dye has not previously been conceivable, owing to the unavoidable and deleterious effects of a few different but coupled processes. First, exciton−exciton annihilation inhibits access to the densities required to surpass the condensation condition to generate macroscopic coherence, where the interparticle separation is less than their de Broglie wavelength. Second, concentration quenching makes it difficult to realize thin films of dyes at the molecular densities needed in solid matrices for polariton generation without compromising drastically the photoluminescence (PL) quantum yield. Third, the inherent structural disorder emerging when dyes aggregate at higher concentrations impedes the large area condensates needed for applications such as polariton-based computations and signal processing. A common solution to all these issues is to dilute the dyes and hence use devices composed of thick organic films.

The recent discovery of fluorescent SMILES material[2,22] has the potential to address these challenges in a straightforward way. Concentration quenching arising from dye aggregation is a long-standing problem that impacts the vast majority of the 100000+ organic dyes in existence and constitutes a general bottleneck in materials creation for many solid-state photonic applications. SMILES provides a universal solution to the problem of aggregation by isolating the dyes ∼15 Å from each other within high-density solids. SMILES are readily formed (Figure 1a) by mixing cationic dyes with the colorless and anion-binding macrocycle, called cyanostar (CS).[2] The macrocycles capture the counteranions associated with the dyes to produce negatively charged building blocks that stack alternately with the dyes in charge-by-charge lattices.[23] Major classes of commercial dyes, including xanthenes, oxazines, styryls, cyanines, and trianguleniums, show fluorescence turn-on in solid state SMILES materials resulting in the brightest known emitters (volume-normalized brightness >7000 M^{-1} cm^{-1}/nm^3) as solids, crystals, thin films, nanoparticles, and doped polymers.[2,24−26] Simple preparation, high photoluminescence quantum yields, and dye−dye isolation promise to circumvent all the issues of annihilation, quenching, and aggregation when organic dyes are dissolved into polymer films.

RESULTS AND DISCUSSION

Here we demonstrate the formation of room-temperature polariton condensation using rhodamine 3B (R3B), a widely used laser dye (with a bandgap ∼2.19 eV, ∼566 nm), composed as a SMILES material. We used the R3B dye as the perchlorate (ClO_4^-) salt, combined it with two mol equiv of cyanostar, and dissolved it in PMMA at a final dye concentration of 10 mM. A thin film of the polymer-SMILES material was produced by spin coating for integration into a Fabry−Perot microcavity structure to demonstrate condensation. The R3B-SMILES film was compared to PMMA-based film incorporating the R3B perchlorate alone (10 mM). Our prior work suggests that the SMILES materials will form charge-by-charge assemblies within the PMMA. The resulting isolation of the R3B dyes in the SMILES based films are highly monomeric.[2] A ∼10× enhancement in PL quantum yield is observed compared to the dye alone and suggests the possibility to implement thinner films than previously studied in the context of molecular polariton condensates.[1,17] A comparison of the absorption and PL for the SMILES complex versus the dye is shown in Supporting Information, Figure S1a,b.

https://doi.org/10.1021/acsphotonics.3c01547
ACS Photonics 2024, 11, 348−355

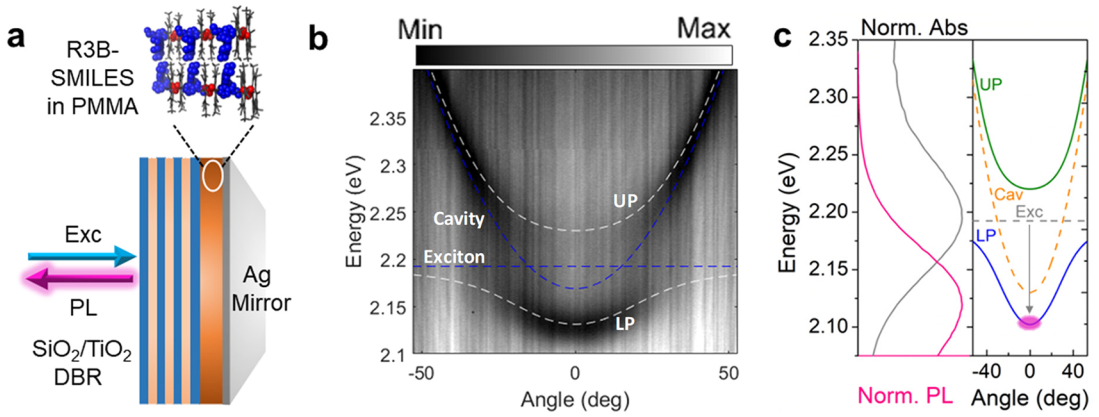

Figure 2. Organic microcavity and dispersion. (a) Schematic of the organic microcavity, consisting of a spin-coated PMMA film (35 ± 5 nm) containing R3B-SMILES sandwiched between a bottom SiO_2/TiO_2 distributed Bragg reflector and a top Ag mirror. (b) Experimental white light reflectivity plots obtained from the cavity sample. The cavity dispersion and the S_{01} main molecular exciton of the R3B-SMILES dispersions are shown in blue. The lower polariton (LP) and upper polariton (UP) dispersions obtained using a coupled oscillator model are shown in white. (c) Left panel shows the normalized absorbance and PL spectra of R3B-SMILES in PMMA film. The right panel shows the dispersion fits for the angle-dependent white light reflectivity plot for the exciton, cavity, and polariton modes. The exciton−cavity detuning (Δ) is chosen so that the lower polariton energy at $k_{||} = 0$ is resonant with the PL maximum to aid radiative pumping.

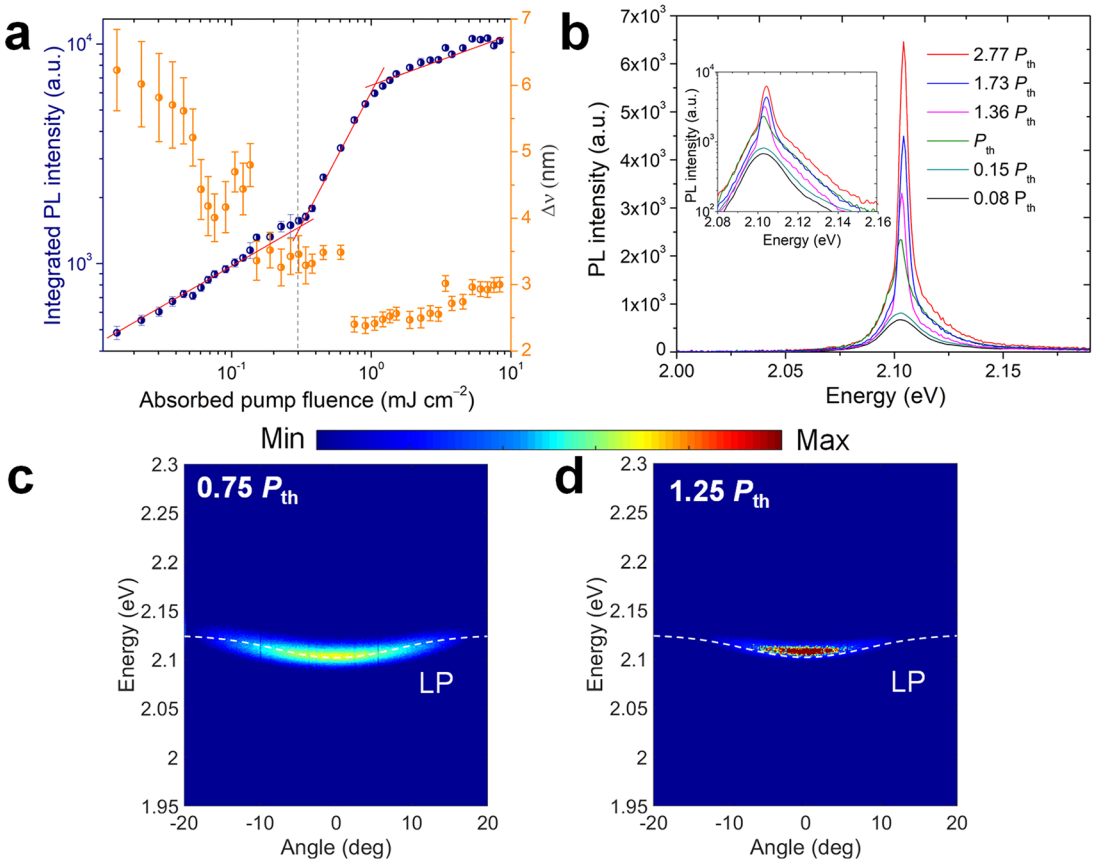

Figure 3. Polariton lasing: (a) Integrated PL intensity (blue circles) along with line width (yellow circles). The threshold is ∼0.2 mJ cm^{-2}. (b) Emission spectra at $k_{||} = 0$ from the SMILES-R3B cavity above and below threshold showing the narrowing of PL beyond P_{th}. Momentum-resolved emission showing the lower polariton dispersion (c) below and (d) above threshold. The emission maximum is blue-shifted above threshold.

The brightness and photostability of thin PMMA films (Figure 1b) composed of R3B-SMILES are superior to those of the R3B alone. The tolerance to photodamage under laser illumination and the reduction in exciton−exciton annihilation of the SMILES films are tested using a 10 kHz pulsed laser at a 530 nm wavelength. The saturation threshold of R3B-SMILES is found to be five times higher than R3B by itself, indicating reduced quenching and photodegradation.

Fortuitously, we observed favorable orientational ordering of the molecular transition dipole moments in the thin PMMA films of R3B-SMILES. Fourier imaging microscopy (FIM) was used to image the emission dipole using PL measurements.[27] The observed Fourier space PL maps observed at the back

https://doi.org/10.1021/acsphotonics.3c01547
ACS Photonics 2024, 11, 348−355

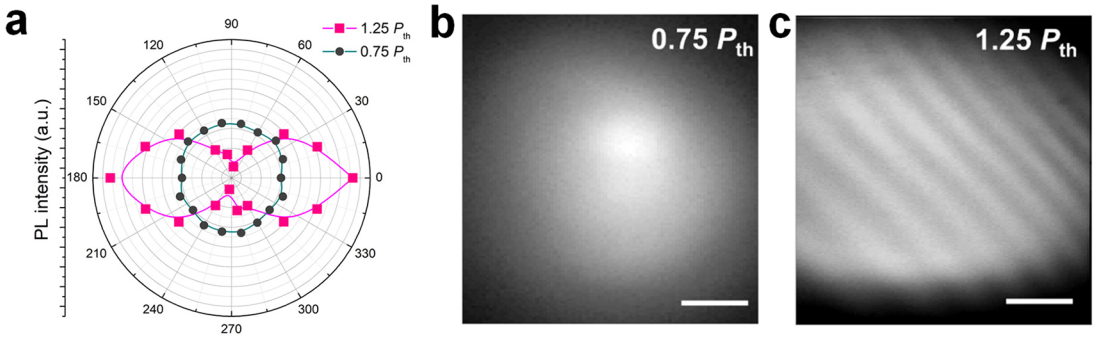

Figure 4. Polarization and spatial coherence. (a) Polar plot depicting the emission intensity with respect to the angle of a polarizer in front of the detector at $0.75P_{th}$ (black) and $1.25P_{th}$ (magenta) excitation power. The emission above the threshold is found to be linearly polarized. Real space PL maps showing (b) homogeneous distribution of PL density for pump power $<P_{th}$ and (c) interference patterns for pump power $>P_{th}$ recorded using a Michelson interferometer configuration. Beyond $\sim 1.2P_{th}$, fringes are observed over the entire condensate area being irradiated by the pump laser and are thus indicative of macroscopic phase coherence throughout the condensate. As the threshold is reached, the emission spot collapses and fringes emerge from the pump center (see Figure S6 for all spatial coherence images with increasing pump fluence). The scale bar corresponds to 5 μm.

focal plane (Figure 1c,d) along with the line cut along the k_y direction (Figure 1e) show the in-plane orientation of the dipoles in the SMILES film. The emission pattern of the R3B SMILES (blue) with a maximum emission at $k_y = 0$ is indicative of the dipoles being aligned in-plane in contrast to the R3B dye (magenta) showing an emission pattern indicative of randomly oriented dipoles.[27] The in-plane orientation of the transition dipole moments in the R3B SMILES film enhances the coupling of the excitons to the cavity photons in a planar Fabry−Perot cavity. Thus, in addition to the photostability and high quantum yield, the ideal dipole orientation provided by the SMILES material offers enhanced light−matter interactions.

The optical cavity (Figure 2a) is composed of a spin-coated, ∼35 nm thin PMMA film of R3B-SMILES (see Methods) sandwiched between a silver top mirror and a bottom SiO_2/TiO_2 distributed Bragg reflector (DBR) on a quartz substrate. The resulting structure supports a Tamm plasmon mode[28,29] with the field maximum overlapping with the spatial position of the SMILES layer, as shown in Supporting Information, Figure S2. The Tamm plasmon cavity showed a loaded Q-factor of ∼150. The experimental white-light reflectivity obtained from the cavity sample using FIM is shown in Figure 2b. Strong coupling of a Tamm cavity mode (∼2.16 eV) with the main molecular exciton of R3B-SMILES (S_{01} at 2.19 eV, as shown in the absorption spectrum plotted as a gray line in the left panel of Figure 2c) resulted in two polariton branches with Rabi splitting, $\hbar\Omega_R \sim 100$ meV. A similar microcavity composed of the same concentration and thickness of the R3B dye alone in the PMMA film as active layer resulted in weak coupling (Figure S1c), despite the negligible difference in excitation and emission energies compared to R3B-SMILES. This difference in performance is attributed to the synergy between high absorption strength and predominantly in-plane dipole orientation in the R3B-SMILES observed from the thin PMMA film.

An important consideration in our design of the Tamm cavity was the detuning between the Tamm plasmon mode and the excitonic transition $\Delta = \omega_{cav} - \omega_{ex}$ at $k_{||} = 0$. The detuning was designed so that the lower polariton at $k_{||} = 0$ was resonant with the PL emission maximum of the dye molecule, thereby ensuring radiative pumping of the lower polariton from the exciton reservoir, a technique that has been shown to be highly efficient in realizing polariton condensation in organic molecular systems.[16,30,31] The detuning was controlled by varying the thickness of the SMILES films.

Following the demonstration of the strong coupling and production of EPs in the R3B-SMILES cavity systems, we carried out studies to determine the onset of condensation. For this purpose, we quantify how PL responds to pump fluence. The cavity was pumped at 2.34 eV, corresponding to the blue edge (reflectivity minimum at normal incidence) of the DBR using a 150 fs laser operating at 10 kHz (see Methods for details). The emission was imaged in momentum space (Figure 3c,d) to study how the dispersion is modified under high-polariton densities. The integrated PL intensity from the LP branch was studied as a function of pump fluence (Figure 3a, blue dots and red line), where a clear threshold behavior is observed. In contrast, the bare R3B cavity showed no nonlinear behavior or threshold (Supporting Information, Figure S1d). In the SMILES cavity, above the threshold for EP condensation at 0.2 mJ cm^{-2} (gray vertical line), a super linear increase in PL intensity is observed along with a collapse in the line width ($\Delta\nu$, yellow dots), indicative of the increase in temporal coherence of the emission. Beyond this threshold, we find a slow power-dependent line-width broadening. This behavior has been discussed extensively in previous reports and has been attributed to phase diffusion stemming from polariton self-interaction within the condensate as well as to condensation within different localized modes.[13,15,32,33] The individual spectra, measured at normal incidence at $k_{||} = 0$, are shown in Figure 3b. Emission from the LP states shows distinct narrowing and almost an order of magnitude increase in peak intensity above condensation threshold.[17] The dispersion of the polariton emission mapped using FIM, below and above the threshold, is shown in Figure 3c and d, respectively. Above the threshold we observe a collapse in momentum space along with a blue shift (Supporting Information, Figure S3), providing another indication of the onset of polariton condensation. The observed threshold is ∼0.2 mJ cm^{-2}, which is comparable to those reported for dye-based cavities with higher Q-factors.[17] The observed blue shift in energy of the PL peak above the condensation threshold (seen in the k-space image Figure 3d and Supporting Information, Figure S3) results from the combination of two effects:[19,34] (i) saturation-induced quenching of the exciton-

https://doi.org/10.1021/acsphotonics.3c01547
ACS Photonics 2024, 11, 348−355

photon coupling, thus lowering the Rabi splitting energy and (ii) renormalization of the cavity mode energy stemming from the change in effective refractive index (n_{eff}) of the cavity when exciting weakly coupled or uncoupled molecules. We also observed the real space emission spot narrowing above threshold (Supporting Information, Figure S4). This narrowing is attributed to the local disorder in organic films that results in localized emission from LP as has been reported previously in such systems.[15]

The polariton condensation observed in the R3B-SMILES microcavity was achieved under ambient conditions, as expected from the large binding energy of Frenkel excitons. The maximum repetition rate of the 2.34 eV pump at which condensation was observed of 10 kHz is one of the highest reported among organic systems. As seen with the pump-dependent study (Figure 1b), the tolerance to higher repetition rate reinforces the advantage of the SMILES platform against the range of processes that typically deteriorate condensation (pump laser-induced heat, O_2 induced bleaching, bimolecular annihilation).

The polarization dependence of the LP emission below the ($0.75P_{th}$) and above the ($1.25P_{th}$) threshold is shown in Figure 4a. The polarization of the emission is observed to be pinned to the polarization of the excitation laser only above the condensation threshold (magenta) with a degree of linear polarization of ∼73%. Shown in Supporting Information, Figure S5 is the emission spectrum collected at different polarizer angles showing clearly the linearly polarized nature of emission from the EP condensate. Similar reports of linearly polarized emission from organic polariton condensates in the past have been attributed to preferential absorption and emission of a specific polarization aligned with the excitation laser.[15]

One of the defining features of condensate formation is the spontaneous appearance of long-range order in the form of spatial coherence.[32,35] This is usually established using an interferometric technique.[32] Here we use a Michelson interferometer in the retroreflector geometry to study the spatial coherence below and above the threshold.[36] Shown in Figure 4b (below threshold) and c (above threshold) are the interference profiles showing clearly the interference pattern above threshold, indicating the onset of spatial coherence in the polariton emission. Below threshold ($0.75P_{th}$), the polariton's PL intensity appears homogeneously distributed over the entire pump spot. Interference fringes at P_{th} begin to emerge (Supporting Information, Figure S6) consistent with the onset of coherent emission from cavity polaritons. With increase in the pump fluence to $>1.2P_{th}$, fringes are readily identified over the entire condensate area illuminated by the pump laser (spot size = 12 μm), which clearly demonstrates the presence of long-range order.

CONCLUSIONS

In summary, we demonstrated a platform for realizing polariton condensates at room temperature using commercially available organic dyes based on SMILES materials. As an indication of the potential for a universal plug-and-play platform, we used rhodamine 3B perchlorate as an archetypical organic laser dye. The thin PMMA films of R3B-SMILES were found to be highly photostable, showing strong tolerance to pump fluence along with in-plane dipole orientation facilitating better coupling to the electromagnetic field in the cavity. The optically active PMMA film of R3B-SMILES was integrated by spin-coating into a metal-DBR hybrid microcavity with a moderate Q-factor (∼150) leading to the formation of polariton condensates. The large spatial coherence and spatial uniformity in the emission point toward low defect density in the R3B-SMILES films, adding to the advantages of the SMILES platform for polariton condensation.

Given that SMILES platform has been shown to work with a wide variety of commercial organic dyes to fully express their bright luminescence in solid state,[2] we foresee the extension of the present work to the large class of commercially available organic cationic dyes. Our results hold promise for achieving a universal solution to the long-standing problem of an optimal emitter and microcavity design to achieve on-demand and room temperature exciton-polariton condensates spanning a wide spectral range. We anticipate these results will make organic polariton condensates more viable for realizing polaritonic devices such as Hamiltonian simulators, ultra-low energy switches and for modifying chemistry in the condensate regime.

METHODS

Formation of R3B-SMILES in Host PMMA. The synthesis of cyanostar has been reported.[2] To prepare the films, a PMMA C2 solution (2% w/w PMMA in chlorobenzene, Kayaku Chem) was diluted by a factor of 2 using chlororobenzene. To this solution was added cyanostar and R3B•ClO_4 (Exciton, Luxottica. Inc.) to make the final concentrations of 20 and 10 mM, respectively. The solution is subjected to vigorous stirring for 48 h at room temperature to undergo formation of the R3B-SMILES assemblies within the PMMA solution. Preparation of solutions of the dye alone involved addition of 10 mM of R3B•ClO_4 to 1 mL of the PMMA C2 solution followed by vigorous stirring for 48 h at room temperature.

Fabrication of Thin Films and Microcavity Samples. The SiO_2/TiO_2 DBR substrates were subjected to O_2 plasma treatment for ∼5 min, which helped to produce better spreading of the R3B-SMILES PMMA solution prior to spinning. The R3B-SMILES solution was then spin-coated by using a three-step recipe. First, about 70 μL of the solution was delivered to the O_2 plasma treated DBR substrate. Second, the substrate was spun at 2000 rpm (t = 15 s) and then 4000 rpm (t = 120 s). These films were subjected to drying in vacuum under constant pressure (2500 Pascal) in the dark at room temperature for ∼48 h. This processing step was found to generate a uniform film thickness across a large area (∼1500−2000 μm^2 along the horizontal plane) estimated from the direct method using a Profilometer (Bruker Dektak-XT). The thickness value estimated from profilometry was ∼35 nm. All these films are then coated with the top mirror by slow evaporation of silver (0.2 Å/s) using the e-beam evaporation technique. We deposited 100 nm of silver mirror on the top for completing the cavity.

Linear Optical Spectroscopy. Measurements of the angle-resolved, white light reflectivity were conducted by using emission from a broadband tungsten halogen lamp. A telescope (1:1 arrangement) with a 100 μm pinhole at the beam waist was used to collimate the beam. The reflected signal was collected using a 50×, 0.8 numerical aperture (NA) objective (same as the incident beam), followed by deflection from a beam splitter to the spectrometer. Solid-state UV−visible measurements on quartz slides were carried out by using a Jasco-760 UV−visible spectrophotometer. Angle-

https://doi.org/10.1021/acsphotonics.3c01547
ACS Photonics 2024, 11, 348−355

resolved PL measurements were performed using a homemade setup comprising a laser coupled with a Princeton Instruments monochromator with a PIXIS: 256 electron-multiplying charge-coupled device (EMCCD) camera. For both momentum-resolved white light and PL measurements, the back focal plane of the imaging objective was projected onto the EMCCD for a single shot dispersion collection. For transient dipole imaging (Figure 1c,d); the entire Fourier circle from the imaging lens was projected onto the EMCCD in an open slit configuration to map in-plane momenta k_x and k_y. A narrow spectral line width was chosen for this imaging around the center emission maxima (±10 nm) for better contrast.

Pump Power-Dependent Photoluminescence Measurements. The pump beam (530 nm) was generated in an optical parametric amplifier (Light Conversion) pumped by the 1030 nm output of an amplified Yb:KGW laser (Light Conversion Carbide), and the pump beam was focused onto the sample by using the 20× objective (NA = 0.40). Our *k*-space setup (with the 10 kHz repetition rate laser) designed for the power-dependent PL experiments was aligned and calibrated with this microscope objective (20×, 0.40 NA) to monitor the collapse of PL intensity around the lower (ground state) *k* vectors. Photoluminescence emission was collected in a reflection configuration using a spectrometer (Princeton Instruments, Acton SpectraPro SP-2500) and charge-coupled device (CCD) camera (Princeton Instruments, PIX 1024B). A 40% DBR transmission (averaged along all angles of incidence) and ∼25% R3B-SMILES absorption was included in estimating the absorbed fluence values at 530 nm (2.3 eV) pump. The residual excitation beam was blocked using a 550 nm long-pass filter. The real space measurements were carried out with an open slit configuration.

Spatial Interferometry. Spatial coherence measurements were made by using a Michelson interferometer configuration. The condensate emission was collected with a 20× objective (NA = 0.40) and directed to a thin nonpolarizing beam splitter. One output arm of the beam splitter consisted of a mirror attached to a micrometer screw gauge stage, and the other consisted of a reflector mirror used to invert the image along both the vertical and horizontal axes. After returning through the beam splitter, the two nearly collimated beams were focused onto a CCD using a f = 12 mm lens, thus providing a ∼47× magnification. A neutral density filter was placed in one arm to equilibrate the intensities, and a 550 nm long-pass filter was used to eliminate any residual pump light.

Coupled Oscillator Model. The coupling of the exciton to a single cavity photonic mode is represented by the following Hamiltonian matrix:[28]

$$H = \begin{pmatrix} E_{ex} - \frac{i\zeta_{ex}}{2} & g \\ g & E_{cav} - \frac{i\zeta_{cav}}{2} \end{pmatrix}$$

Wherein g is the coupling strength of the cavity mode with the excitonic resonance and gives the Rabi splitting of interaction as stated in the main text. Both ζ_{ex} and ζ_{cav} are the line widths (fwhm) of the exciton and cavity modes. We solve for the Eigen modes of the above Hamiltonian to get the polariton branch dispersion as a function of in-plane momentum (angles) and fit these with our experimental data for upper and lower polaritonic branches. We also extract Hopfield coefficients from the same interacting Hamiltonian as shown below:

$$|\mathrm{UPB}\rangle = C(k)|\mathrm{exciton}\rangle + X(k)|\mathrm{photon}\rangle$$

$$|\mathrm{LPB}\rangle = X(k)|\mathrm{exciton}\rangle - C(k)|\mathrm{photon}\rangle$$

Here, $C(k)$ and $X(k)$ are Hopfield coefficients describing the photon and exciton fraction in the upper (UPB) and lower polariton branches (LPB).

■ ASSOCIATED CONTENT

Data Availability Statement

All data will be provided by the corresponding authors upon reasonable request.

Supporting Information

The Supporting Information is available free of charge at https://pubs.acs.org/doi/10.1021/acsphotonics.3c01547.

Comparison of solution and thin film absorption; White light reflectivity for the bare dye molecule; Electric field calculations of cavity structure; Power-dependent blue-shift of the lower polariton (LP) photoluminescence; Real space photoluminescence of R3B-SMILES cavity below and above threshold; Angle-dependent polarized microcavity PL of the condensate above threshold and comparison of real space interference graphs for R3B-SMILES microcavity (PDF)

■ AUTHOR INFORMATION

Corresponding Authors

Sitakanta Satapathy − *Department of Physics, Center for Discovery and Innovation, The City College of New York, New York, New York 10031, United States*; Email: sitakant2101@gmail.com

Vinod M. Menon − *Department of Physics, Center for Discovery and Innovation, The City College of New York, New York, New York 10031, United States; The PhD Program in Physics, The Graduate Center of the City University of New York, New York, New York 10016, United States*; orcid.org/0000-0002-9725-6445; Email: vmenon@ccny.cuny.edu

Authors

Prathmesh Deshmukh − *Department of Physics, Center for Discovery and Innovation, The City College of New York, New York, New York 10031, United States; The PhD Program in Physics, The Graduate Center of the City University of New York, New York, New York 10016, United States*

Evripidis Michail − *Photonics Initiative, Advanced Science Research Center, City University of New York, New York, New York 10031, United States*

Andrew H. Olsson − *Department of Chemistry, Indiana University, Bloomington, Indiana 47405, United States*

Rezlind Bushati − *Department of Physics, Center for Discovery and Innovation, The City College of New York, New York, New York 10031, United States; The PhD Program in Physics, The Graduate Center of the City University of New York, New York, New York 10016, United States*

Ravindra Kumar Yadav − *Department of Physics, Center for Discovery and Innovation, The City College of New York, New York, New York 10031, United States*

https://doi.org/10.1021/acsphotonics.3c01547
ACS Photonics 2024, 11, 348−355

Mandeep Khatoniar − *Department of Physics, Center for Discovery and Innovation, The City College of New York, New York, New York 10031, United States; The PhD Program in Physics, The Graduate Center of the City University of New York, New York, New York 10016, United States*

Junsheng Chen − *Nano-Science Center & Department of Chemistry, University of Copenhagen, 2100 Copenhagen, Denmark*

George John − *Department of Chemistry, Center for Discovery and Innovation, The City College of New York, New York, New York 10031, United States;* orcid.org/0000-0002-0382-1256

Bo W. Laursen − *Nano-Science Center & Department of Chemistry, University of Copenhagen, 2100 Copenhagen, Denmark*

Amar H. Flood − *Department of Chemistry, Indiana University, Bloomington, Indiana 47405, United States;* orcid.org/0000-0002-2764-9155

Matthew Y. Sfeir − *The PhD Program in Physics, The Graduate Center of the City University of New York, New York, New York 10016, United States; Photonics Initiative, Advanced Science Research Center, City University of New York, New York, New York 10031, United States;* orcid.org/0000-0001-5619-5722

Complete contact information is available at: https://pubs.acs.org/10.1021/acsphotonics.3c01547

Author Contributions

V.M.M. and S.S. conceived the idea and designed the experiments. P.D. and S.S. contributed equally to this manuscript. S.S. made the samples including thin film optimization, cavity device fabrication, optical characterization, and Raman measurements. P.D. setup the optics for all the power dependent measurements. R.B., M.E., and M.Y.S. assisted in designing the optics. P.D., M.E., and S.S. performed the power dependent measurements with inputs from M.Y.S. S.S. and P.D. analyzed the data and wrote the manuscript with input from V.M.M., A.H.F., and B.W.L. The synthesis and characterization of cyanostar and SMILES materials was performed by J.C. and A.H.O. All authors discussed the results and commented on the manuscript. All authors have given approval to the final version of the manuscript.

Funding

V.M.M., S.S., and R.K.Y. were supported by the U.S. Air Force Office of Scientific Research − MURI Grant FA9550-22-1-0317. S.S., P.D., and R.B. acknowledge support from the US National Science Foundation (NSF− QTAQS program OMA−1936351. M.Y.S. work was supported by the U.S. Department of Energy, Office of Science, Office of Basic Energy Sciences under Award No. DE-SC0022036. A.H.O. and A.H.F. acknowledge support from the U.S. National Science Foundation (DMR-2118423).

Notes

The authors declare the following competing financial interest(s): A.F. and B.L. are cofounders in Halophore, Inc. R.Y., S.S., P.D., V.M., B.L., and A.F. have filed a provisional patent application.

■ ACKNOWLEDGMENTS

The authors acknowledge the use of the nanofabrication and imaging facility at ASRC, CUNY.

■ REFERENCES

(1) Keeling, J.; Kéna-Cohen, S. Bose−Einstein condensation of exciton-polaritons in organic microcavities. *Annu. Rev. Phys. Chem.* **2020**, *71*, 435−459.

(2) Benson, C. R.; Kacenauskaite, L.; VanDenburgh, K. L.; Zhao, W.; Qiao, B.; Sadhukhan, T.; Pink, M.; Chen, J.; Borgi, S.; Chen, C.-H.; et al. Plug-and-Play Optical Materials from Fluorescent Dyes and Macrocycles. *Chem.* **2020**, *6*, 1978−1997.

(3) Sanvitto, D.; Kena-Cohen, S. The road towards polaritonic devices. *Nat. Mater.* **2016**, *15*, 1061−1073.

(4) Carusotto, I.; Ciuti, C. Quantum fluids of light. *Rev. Mod. Phys.* **2013**, *85*, 299−366.

(5) Amo, A.; Lefrere, J.; Pigeon, S.; Adrados, C.; Ciuti, C.; Carusotto, I.; Houdre, R.; Giacobino, E.; Bramati, A. Superfluidity of polaritons in semiconductor microcavities. *Nat. Phys.* **2009**, *5*, 805−810.

(6) Lerario, G.; Fieramosca, A.; Barachati, F.; Ballarini, D.; Daskalakis, K. S.; Dominici, L.; De Giorgi, M.; Maier, S. A.; Gigli, G.; Kena-Cohen, S.; Sanvitto, D. Room-temperature superfluidity in a polariton condensate. *Nat. Phys.* **2017**, *13*, 837−841.

(7) Berloff, N. G.; Silva, M.; Kalinin, K.; Askitopoulos, A.; Topfer, J. D.; Cilibrizzi, P.; Langbein, W.; Lagoudakis, P. G. Realizing the classical XY Hamiltonian in polariton simulators. *Nat. Mater.* **2017**, *16*, 1120−1126.

(8) Christopoulos, S.; von Hogersthal, G. B. H.; Grundy, A. J. D.; Lagoudakis, P. G.; Kavokin, A. V.; Baumberg, J. J.; Christmann, G.; Butte, R.; Feltin, E.; Carlin, J.-F.; Grandjean, N. Room-Temperature Polariton Lasing in Semiconductor Microcavities. *Phys. Rev. Lett.* **2007**, DOI: 10.1103/PhysRevLett.98.126405.

(9) Anton-Solanas, C.; Waldherr, M.; Klaas, M.; Suchomel, H.; Harder, T. H.; Cai, H.; Sedov, E.; Klembt, S.; Kavokin, A. V.; Tongay, S.; Watanabe, K.; Taniguchi, T.; Hofling, S.; Schneider, C. Bosonic condensation of exciton−polaritons in an atomically thin crystal. *Nat. Mater.* **2021**, *20*, 1233−1239.

(10) Zhao, J.; Su, R.; Fieramosca, A.; Zhao, W.; Du, W.; Liu, X.; Diederichs, C.; Sanvitto, D.; Liew, T. C. H.; Xiong, Q. Ultralow Threshold Polariton Condensate in a Monolayer Semiconductor Microcavity at Room Temperature. *Nano Lett.* **2021**, *21*, 3331−3339.

(11) Su, R.; Fieramosca, A.; Zhang, Q.; Nguyen, H. S.; Deleporte, E.; Chen, Z.; Sanvitto, D.; Liew, T. C. H.; Xiong, Q. Perovskite semiconductors for room-temperature exciton-polaritonics. *Nat. Mater.* **2021**, *20*, 1315−1324.

(12) Deng, H.; Haug, H.; Yamamoto, Y. Exciton-polariton Bose−Einstein condensation. *Rev. Mod. Phys.* **2010**, *82*, 1489−1537.

(13) Kéna-Cohen, S.; Forrest, S. R. Room-temperature polariton lasing in an organic single-crystal microcavity. *Nat. Photonics* **2010**, *4*, 371−375.

(14) Plumhof, J. D.; Stöferle, T.; Mai, L.; Scherf, U.; Mahrt, R. F. Room-temperature Bose−Einstein condensation of cavity exciton−polaritons in a polymer. *Nat. Mater.* **2014**, *13*, 247−252.

(15) Daskalakis, K. S.; Maier, S. A.; Murray, R.; Kéna-Cohen, S. Nonlinear interactions in an organic polariton condensate. *Nat. Mater.* **2014**, *13*, 271−278.

(16) Grant, R. T.; Michetti, P.; Musser, A. J.; Gregoire, P.; Virgili, T.; Vella, E.; Cavazzini, M.; Georgiou, K.; Galeotti, F.; Clark, C.; Clark, J.; Silva, C.; Lidzey, D. G. Efficient Radiative Pumping of Polaritons in a Strongly Coupled Microcavity by a Fluorescent Molecular Dye. *Adv. Opt Mater.* **2016**, *4*, 1615−1623.

(17) Cookson, T.; Georgiou, K.; Zasedatelev, A.; Grant, R. T.; Virgili, T.; Cavazzini, M.; Galeotti, F.; Clark, C.; Berloff, N. G.; Lidzey, D. G.; Lagoudakis, P. G. A Yellow Polariton Condensate in a Dye Filled Microcavity. *Adv. Opt Mater.* **2017**, *5*, 1700203.

(18) Rajendran, S. K.; Wei, M.; Ohadi, H.; Ruseckas, A.; Turnbull, G. A.; Samuel, I. D. W. Low Threshold Polariton Lasing from a Solution-Processed Organic Semiconductor in a Planar Microcavity. *Adv. Opt Mater.* **2019**, *7*, 1801791.

(19) Yagafarov, T.; Sannikov, D.; Zasedatelev, A.; Georgiou, K.; Baranikov, A.; Kyriienko, O.; Shelykh, I.; Gai, L.; Shen, Z.; Lidzey, D.;

Lagoudakis, P. Mechanisms of blueshifts in organic polariton condensates. *Commun. Phys.* **2020**, *3*, 18.
(20) Wei, M.; Rajendran, S. K.; Ohadi, H.; Tropf, L.; Gather, M. C.; Turnbull, G. A.; Samuel, I. D. W. Low-threshold polariton lasing in a highly disordered conjugated polymer. *Optica* **2019**, *6*, 1124−1129.
(21) Dietrich, C. P.; Steude, A.; Tropf, L.; Schubert, M.; Kronenberg, N. M.; Ostermann, K.; Höfling, S.; Gather, M. C. An exciton-polariton laser based on biologically produced fluorescent protein. *Sci. Adv.* **2016**, *2*, e1600666.
(22) Lee, S.; Chen, C. H.; Flood, A. H. A pentagonal cyanostar macrocycle with cyanostilbene CH donors binds anions and forms dialkylphosphate [3] rotaxanes. *Nat. Chem.* **2013**, *5*, 704−710.
(23) Haketa, Y.; Sasaki, S.; Ohta, N.; Masunaga, H.; Ogawa, H.; Mizuno, N.; Araoka, F.; Takezoe, H.; Maeda, H. Oriented salts: dimension-controlled charge-by-charge assemblies from planar receptor−anion complexes. *Angew. Chem.* **2010**, *122* (52), 10277−10281.
(24) Chen, J.; Stenspil, S. G.; Kaziannis, S.; Kacenauskaite, L.; Lenngren, N.; Kloz, M.; Flood, A. H.; Laursen, B. W. Quantitative Energy Transfer in Organic Nanoparticles Based on Small-Molecule Ionic Isolation Lattices for UV Light Harvesting. *ACS Appl. Nano Mater.* **2022**, *5*, 13887−13893.
(25) Chen, J.; Fateminia, S. M. A.; Kacenauskaite, L.; Bærentsen, N.; Grønfeldt Stenspil, S.; Bredehoeft, J.; Martinez, K. L.; Flood, A. H.; Laursen, B. W. Ultrabright Fluorescent Organic Nanoparticles Based on Small-Molecule Ionic Isolation Lattice. *Angew. Chem. Int. Ed.* **2021**, *60*, 9450−9458.
(26) Kacenauskaite, L.; Stenspil, S. G.; Olsson, A. H.; Flood, A. H.; Laursen, B. W. Universal Concept for Bright, Organic, Solid-State Emitters Doping of Small-Molecule Ionic Isolation Lattices with FRET Acceptors. *J. Am. Chem. Soc.* **2022**, *144*, 19981−19989.
(27) Schuller, J. A.; Karaveli, S.; Schiros, T.; He, K.; Yang, S.; Kymissis, I.; Shan, J.; Zia, R. Orientation of luminescent excitons in layered nanomaterials. *Nat. Nanotechnol.* **2013**, *8*, 271−276.
(28) Sasin, M. E.; Seisyan, R. P.; Kalitteevski, M. A.; Brand, S.; Abram, R. A.; Chamberlain, J. M.; Egorov, A. Y.; Vasil'ev, A. P.; Mikhrin, V. S.; Kavokin, A. V. Tamm plasmon polaritons: Slow and spatially compact light. *Appl. Phys. Lett.* **2008**, *92*, 251112.
(29) Afinogenov, B. I.; Bessonov, V. O.; Nikulin, A. A.; Fedyanin, A. A. Observation of hybrid state of Tamm and surface plasmon-polaritons in one-dimensional photonic crystals. *Appl. Phys. Lett.* **2013**, *103*, No. 061112.
(30) Grant, R. T.; Michetti, P.; Musser, A. J.; Gregoire, P.; Virgili, T.; Vella, E.; Cavazzini, M.; Georgiou, K.; Galeotti, F.; Clark, C.; et al. Efficient Radiative Pumping of Polaritons in a Strongly Coupled Microcavity by a Fluorescent Molecular Dye. *Adv. Opt. Mater.* **2016**, *4*, 1615−1623.
(31) Ishii, T.; Miyata, K.; Mamada, M.; Bencheikh, F.; Mathevet, F.; Onda, K.; Kéna-Cohen, S.; Adachi, C. Low-Threshold Exciton-Polariton Condensation via Fast Polariton Relaxation in Organic Microcavities. *Adv. Opt. Mater.* **2022**, *10*, 2102034.
(32) Kasprzak, J.; Richard, M.; Kundermann, S.; Baas, A.; Jeambrun, P.; Keeling, J. M. J.; Marchetti, F. M.; Szymańska, M. H.; André, R.; Staehli, J. L.; et al. Bose−Einstein condensation of exciton polaritons. *Nature* **2006**, *443*, 409−414.
(33) Porras, D.; Tejedor, C. Linewidth of a polariton laser: Theoretical analysis of self-interaction effects. *Phys. Rev. B* **2003**, *67*, 161310.
(34) Mazza, L.; Kéna-Cohen, S.; Michetti, P.; la Rocca, G. C. Microscopic theory of polariton lasing via vibronically assisted scattering. *Phys. Rev. B Condens Matter Mater. Phys.* **2013**, *88*, No. 075321.
(35) Deng, H.; Solomon, G.; Hey, R.; Ploog, K.; Yamamoto, Y. Spatial Coherence of a Polariton Condensate. *Phys. Rev. Lett.* **2007**, *99*, 126403.
(36) Daskalakis, K. S.; Maier, S. A.; Kéna-Cohen, S. Spatial Coherence and Stability in a Disordered Organic Polariton Condensate. *Phys. Rev. Lett.* **2015**, *115*, No. 035301.

Recommended by ACS

Damage Evolution and Acoustic Emission Characteristics of Sandstone under Freeze–Thaw Cycles
Chuangye Wang, Huangjin Zhu, *et al.*
JANUARY 19, 2024
ACS OMEGA
READ

Experimental Investigation on the Influence of Wave Impedance on Dynamic Mechanical Response of Granites undergone High Temperature
Weiyu Li, Xin Gao, *et al.*
NOVEMBER 02, 2023
ACS OMEGA
READ

Specificity of the Thermal Stability and Reactivity of Two-Dimensional Layered Cu–Fe Sulfide-Mg-Based Hydroxide Compounds (Valleriites)
Maxim N. Likhatski, Yuri L. Mikhlin, *et al.*
SEPTEMBER 18, 2023
ACS OMEGA
READ

Measuring the Influence of Seedling Age and Nutrient Sources on the Performance of Sweet Corn (*Zea mays* L.) under Temperate Climatic Conditions
Bisma Jan, Ayman El Sabagh, *et al.*
MAY 16, 2023
ACS OMEGA
READ

Get More Suggestions >

https://doi.org/10.1021/acsphotonics.3c01547
ACS Photonics 2024, 11, 348−355